Chapter 5

ESTIMATING RELATIVE PERMITTIVITY AND SIZE OF INTERPHASE

5.1 INTRODUCTION

The preceding chapter discussed the mechanism of interphase formation and its relationship to the material properties of epoxy alumina nanocomposites. Apart from qualitative analysis, quantitative analysis of the interphase is crucial for optimizing the usage of nanofillers and obtaining customized material properties. This chapter will discuss a novel method for assessing the permittivity and thickness of interphase in epoxy-based nanocomposites. A finite element-based numerical model is developed to estimate the effective permittivity of composites for different values of assumed interphase parameters (i.e., thickness and permittivity). Bisection method-based algorithm is developed to assign actual thickness and permittivity to interphase based on best fit of experimental and simulated results.

5.2 METHODOLOGY

The effective permittivity of nanocomposites is estimated using finite element analysis (FEA). The various steps of FEA are depicted in Figure 5.1. The analysis is carried out using the COMSOL multi-physics software. The following subsection discusses numerical modeling in greater detail.

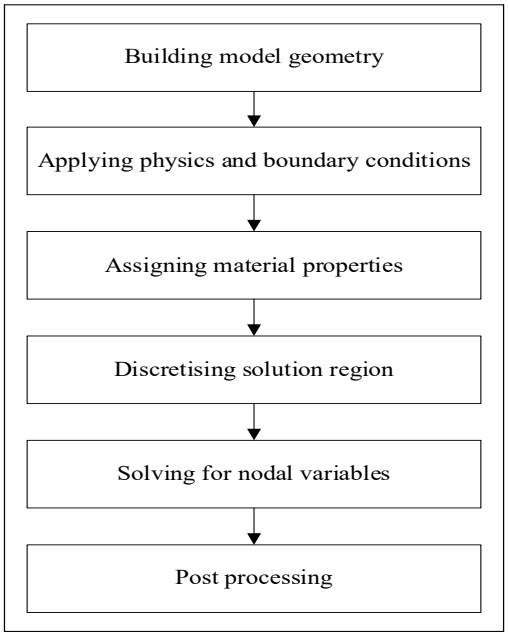

Figure 5.1 Flow diagram for performing numerical simulation using FEM

5.2.1 Building model geometry and selection of unit cell

Uniformity of filler dispersion and periodicity across sample cross section is ascertained in chapter 4 (section 4.2.1). This enables us to perform finite element analysis on a unit cell model. As illustrated in Table 4.1, the average inter-particle distance is 198 nm in the actual synthesized sample at a filler concentration of 1 vol. %. To ensure that the unit cell is a three-dimensional statistically representative volume element of actual synthesized samples, the spacing between neighboring particle centers in unit cell is set to 198 nm. In Figure 5.2a, the unit cell representing the required particle volume fraction is depicted. Each particle is spherical, placed at one of the cube's eight corners, and surrounded by an interphase zone. Figure 5.2a, 5.2b, and 5.2c highlight the nanoparticle, interphase, and base polymer phases, respectively. Symbols pertaining to the unit cell are shown in Table 5.1.

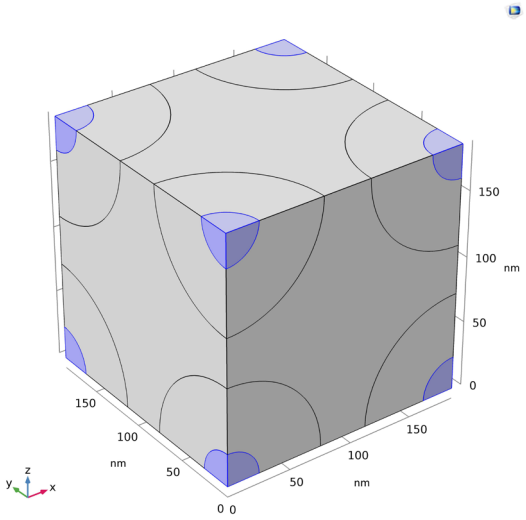

(a)

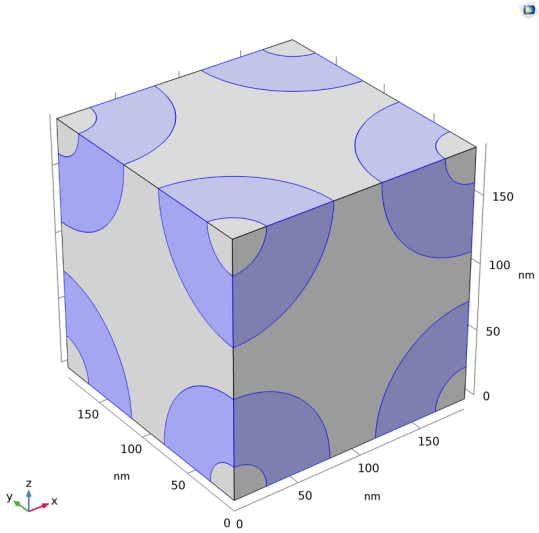

(b)

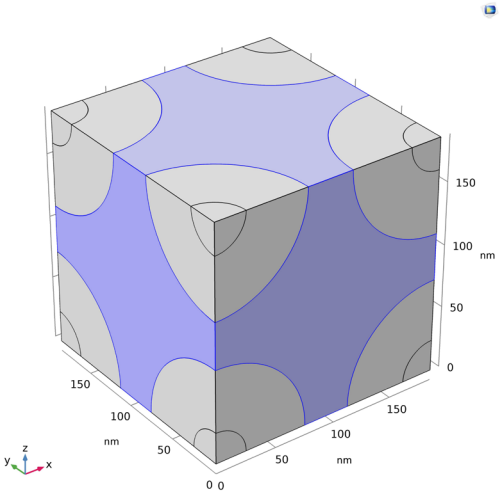

(c)

Figure 5.2 Highlighted region in a simple cubic unit cell (a) nanoparticle (b) interphase (c) base polymer

Table 5.1 List of symbols or notations associated with unit cell

Notation	Explanation
r_p	radius of particle (r_p=25nm)
r_i	radius of interphase
Th	thickness of interphase
D	length of side of the cube of unit cell model

This model considers the overlapping of interphases, and the geometrical regimes are categorized into four different cases as discussed below:

Case 1. Non-Overlapping interphase ($r_i \leq \frac{D}{2}$)

Case 2. Interphase overlap through edges of the cube ($\frac{D}{2} \leq r_i \leq \frac{D}{\sqrt{2}}$)

Case 3. Interphase overlap through face diagonal of the cube ($\frac{D}{\sqrt{2}} \leq r_i \leq \frac{\sqrt{3}}{2} D$)

Case 4. Interphase expands into the entire polymer matrix ($r_i \geq \frac{\sqrt{3}}{2} D$)

5.2.2 Applying physics and boundary conditions

For this numerical analysis, Electrostatics (es) with AC/DC module of the COMSOL multi-physics software is used. To determine the potential distribution within a dielectric sample, Electrostatics (es) physics solves the following equations:

$$E = -\nabla V \tag{5.1}$$

$$\nabla.(\epsilon_0 \epsilon_r E) = 0 \tag{5.2}$$

where,

V= Electric potential

E= Electric field

ϵ_0 = Permittivity of the free space

ϵ_r = Relative permittivity of the medium.

Zero charge boundary condition is applied at all the faces of cube except cubic faces/or boundaries representing high voltage and ground electrode. Zero charge boundary condition means no displacement field can penetrate the boundary ($n.D = 0$).

5.2.3 Assignment of material properties

The host polymer in cubical block is assigned the relative permittivity of epoxy resin (ϵ_r=4), and the filler is assigned the relative permittivity value of alumina (ϵ_r=10). Interphase does not have a known relative permittivity or thickness. Thus, the finite element analysis is started with an assumed range of interphase thickness and relative permittivity. Later parts discuss the upper and lower bounds for presumed relative permittivity, as well as how to estimate the real size and relative permittivity of interphase.

5.2.4 Calculation of effective permittivity

Effective permittivity of the dielectric sample is calculated by considering the average values of dielectric displacement and electric field intensity. A constitutive relationship between dielectric displacement vector and electric field intensity is shown in (5.3).

$$\langle D \rangle = \varepsilon \langle E \rangle \tag{5.3}$$

where, $\langle E \rangle$ is defined as the average of the electric field over the volume V of the unit cell, $\langle D \rangle$ is defined as the average of the electric displacement field over the volume V of the unit cell and ε is the effective permittivity of the medium.

$$\varepsilon = \varepsilon_o \times \varepsilon_r \tag{5.4}$$

where, ε_o is the permittivity of the free space and ε_r is the absolute relative permittivity of the medium. The relative permittivity of the nanocomposite material is calculated using (5.5).

$$\varepsilon_r = \frac{1}{\varepsilon_\circ}\frac{\langle D \rangle}{\langle E \rangle} \tag{5.5}$$

The average electric field of the unit cell is calculated as,

$$\langle E \rangle = \frac{1}{V}\iiint_{vol} E(x,y,z)dv \tag{5.6}$$

And electric displacement field of the unit cell is calculated as,

$$\langle D \rangle = \frac{1}{V}\iiint_{vol} D(x,y,z)dv \tag{5.7}$$

where, $E(x,y,z)$ and $D(x,y,z)$ are electric field and displacement field in Cartesian co-ordinates x,y,z.

$$D(x,y,z) = \sqrt{(D_x)^2 + (D_y)^2 + (D_z)^2} \tag{5.8}$$

$$E(x,y,z) = \sqrt{(E_x)^2 + (E_y)^2 + (E_z)^2} \tag{5.9}$$

where, E_x, E_y, E_z and D_x, D_y, D_z are components of electric field and electric displacement field respectively. Post-processing results of electric field and electric displacement field inside the model are shown in Figure 5.3a and 5.3b respectively.

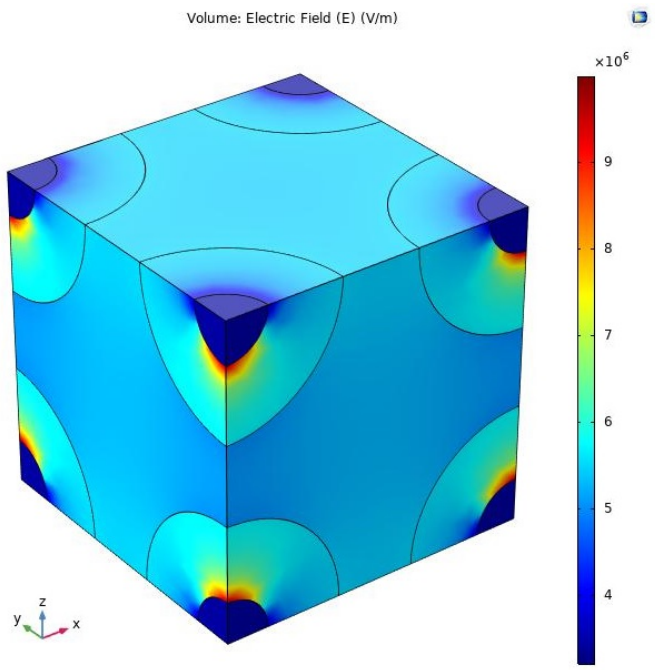

(a)

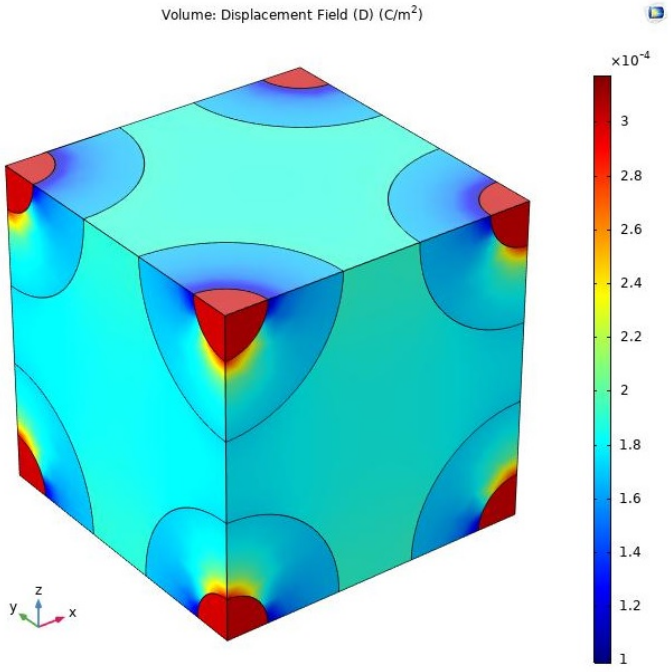

(b)

Figure 5.3 Plots from simulation studies (a) electric field intensity (E), (b) displacement field (D)

5.3 VALIDATION OF FINITE ELEMENT ANALYSIS

To verify the validity of the physics and boundary conditions mentioned previously for given sub domain properties and to determine the accuracy of numerical computations using finite element analysis, an analytical solution for a simple parallel plane geometry is obtained and then compared to a solution obtained using finite element analysis. A parallel plate capacitor with two layers of differing permittivity dielectric materials is shown in Figure 5.4. Teflon ($\varepsilon_r = 4.2$) and glass ($\varepsilon_r = 2.1$) were chosen for the first and second layers, respectively. Each layer has a surface area of 50 cm^2 and a thickness of 2 cm. The procedure for calculating effective permittivity and electrical field distribution analytically is as follows:

If the fringing effect is ignored, only the normal component of the electric field and flux density exist in both dielectric layers. With this assumption the potential distribution across the dielectric layers is given by (5.10).

$$V = V_1 + V_2 \tag{5.10}$$

Where V, V_1, and V_2 represent the applied electric potential across the series combination, the potential across layer 1, and the potential across layer 2.

If E_1 and E_2 represent the electric fields in layer 1 and layer 2, respectively, (5.10) may be rewritten as:

$$V = E_1 d_1 + E_2 d_2 \tag{5.11}$$

The mean value of the electric field is calculated as illustrated in (5.12):

$$\frac{V}{d} = E_1 \frac{d_1}{d} + E_2 \frac{d_2}{d} \tag{5.12}$$

$$< E >= E_1 \frac{d_1}{d} + E_2 \frac{d_2}{d} \tag{5.13}$$

$$D_1 = D_2 =< D > \tag{5.14}$$

Normal component of electric flux densities in layer 1 and layer 2 is given by:

$$D_1 = \varepsilon_1 E_1 = D_2 = \varepsilon_2 E_2 \tag{5.15}$$

The effective permittivity can be calculated by dividing (5.13) by $< D >$ as seen below in (5.16).

$$\frac{< E >}{< D >} = \frac{E_1 \frac{d_1}{d}}{< D >} + \frac{E_2 \frac{d_2}{d}}{< D >} \tag{5.16}$$

$$\frac{1}{\varepsilon_{eff}} = \frac{v_{f1}}{\varepsilon_1} + \frac{v_{f2}}{\varepsilon_2} \tag{5.17}$$

$$\frac{1}{\varepsilon_{r_{eff}}} = \frac{v_{f1}}{\varepsilon_{r1}} + \frac{v_{f2}}{\varepsilon_{r2}} \tag{5.18}$$

The effective relative permittivity of two-layer dielectric system is obtained by simplifying (5.18) and shown in (5.19).

$$\varepsilon_{reff} = \frac{\varepsilon_{r1}\varepsilon_{r2}}{\varepsilon_{r1} v_{f2} + \varepsilon_{r2} v_{f1}} \tag{5.19}$$

where ε_{r1} and ε_{r2} are the relative permittivities of the first and second layer respectively and v_{f1} and v_{f2} are volume fraction of the first and second layer respectively.

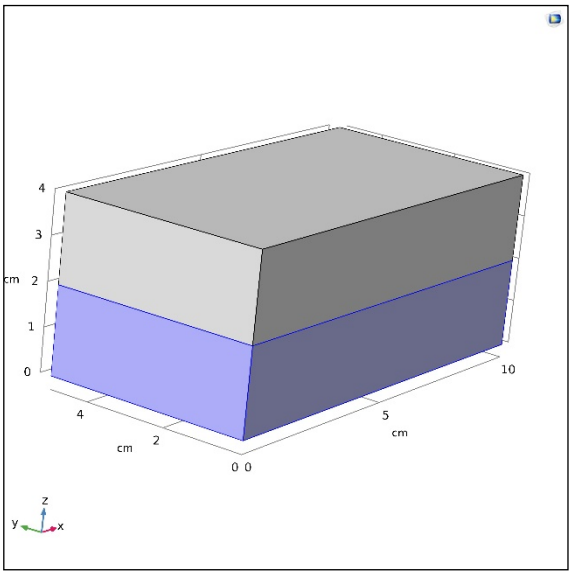

Figure 5.4 Capacitor with two different dielectric materials

Using (5.11) and (5.15) electric field in two layers can be computed as shown in (5.20) and (5.22).

$$E_1 = \frac{V\varepsilon_{r2}}{\varepsilon_{r1}d_2 + \varepsilon_{r2}d_1} \tag{5.20}$$

$$E_2 = \frac{V\varepsilon_{r1}}{\varepsilon_{r2}d_1 + \varepsilon_{r1}d_2} \tag{5.21}$$

Furthermore, for the same example described previously, the effective permittivity and electric field distribution are computed using COMSOL (a finite element method-based software). Figure 5.5 shows the potential and electric field distributions in two dielectric layers obtained using numerical simulation. For a 10 V applied voltage across the series-connected dielectric layers, Table 5.2 shows the various quantities obtained using analytical solution and FEA.

This analysis demonstrates that the modeling procedure in terms of physics, domain properties, and boundary conditions is correct for obtaining an acceptable numerical solution.

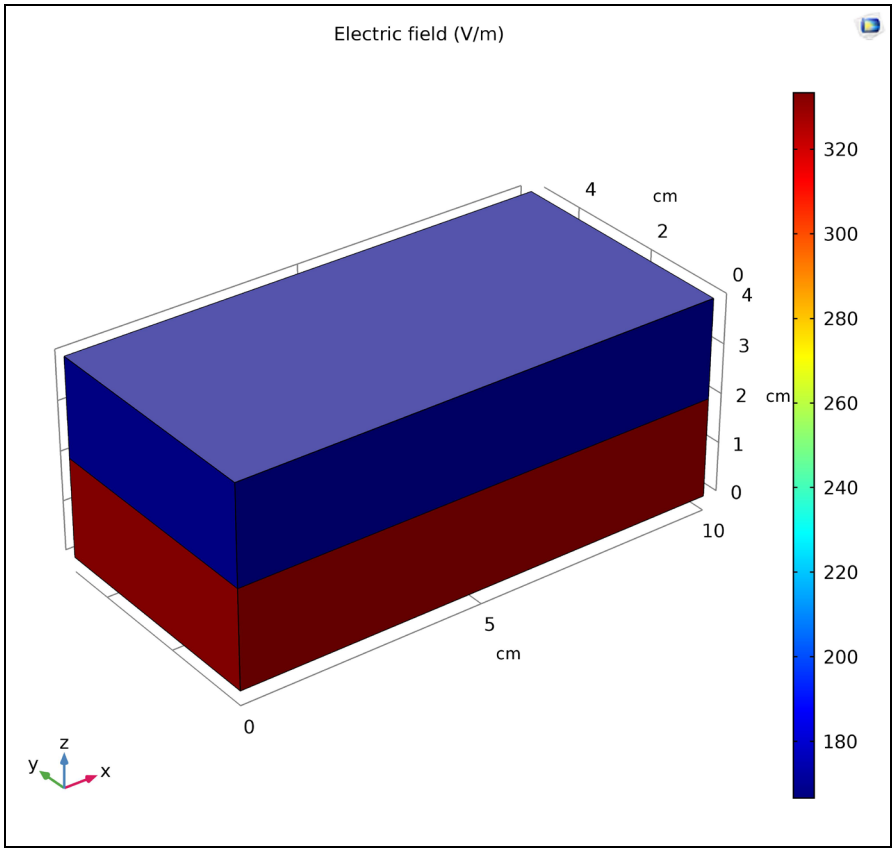

Figure 5.5 Electric field distribution in two layer dielectric system

Table 5.2 Comparison of analytical and numerically computed values

Quantity	**Computed values**		**% Error**
	Analytical	**Numerical**	
Electric field in Teflon/or layer 1 (E_1)	167.67 (V/m)	166.57 (V/m)	0.06
Electric field in Glass/or layer 2 (E_2)	333.33 (V/m)	333.13 (V/m)	0.06
Mean electric flux density ($< D >$)	6.20×10^{-9} (C/m^2)	6.14×10^{-9} (C/m^2)	0.96
Mean electric field ($< E >$)	250 (V/m)	249.85	0.06
Effective relative permittivity (ε_{eff})	2.80	2.78	0.71

5.4 DETERMINATION OF INTERPHASE PERMITTIVITY USING BISECTION METHOD ALGORITHM

5.4.1 Bisection method

The bisection method is a successive approximation method that iteratively narrows down the interval containing the root of any continuous function $f(x) = 0$. This method repeatedly bisects the interval and then selects a sub-interval in which the root must lie for further processing. The bisection method is applicable for numerically solving the equation $f(x) = 0$, where $f(x)$ is a continuous function defined over the interval $[a, b]$ and here $f(a)$ and $f(b)$ are the two values having opposite sign to each other, such the root p must lie between a and b, with $f(p) = 0$. This method bisects the interval into two at every step by determining the midpoint $p = (a + b) / 2$ of the interval $[a, b]$ and calculates the value of the function $f(p)$ at that particular point. The root lies between a and p, if $f(a)$ and $f(p)$ have opposite signs to each other and hence, this method will select p as a new value of b. However, it may also happen that $f(p)$ and $f(b)$ have opposite signs to each other, then the root lies in between p and b, and hence this method will select p as a new value of a. In both cases, the new function value $f(a)$ and $f(b)$ have opposite sign to each other, and the bisection method will now be applied to this smaller interval. In this way, an interval that contains the root is reduced in width by 50% at every step. The process will be continued until the solution is converged [98]. An iterative mechanism that leads to a conversed solution is depicted in Figure 5.6.

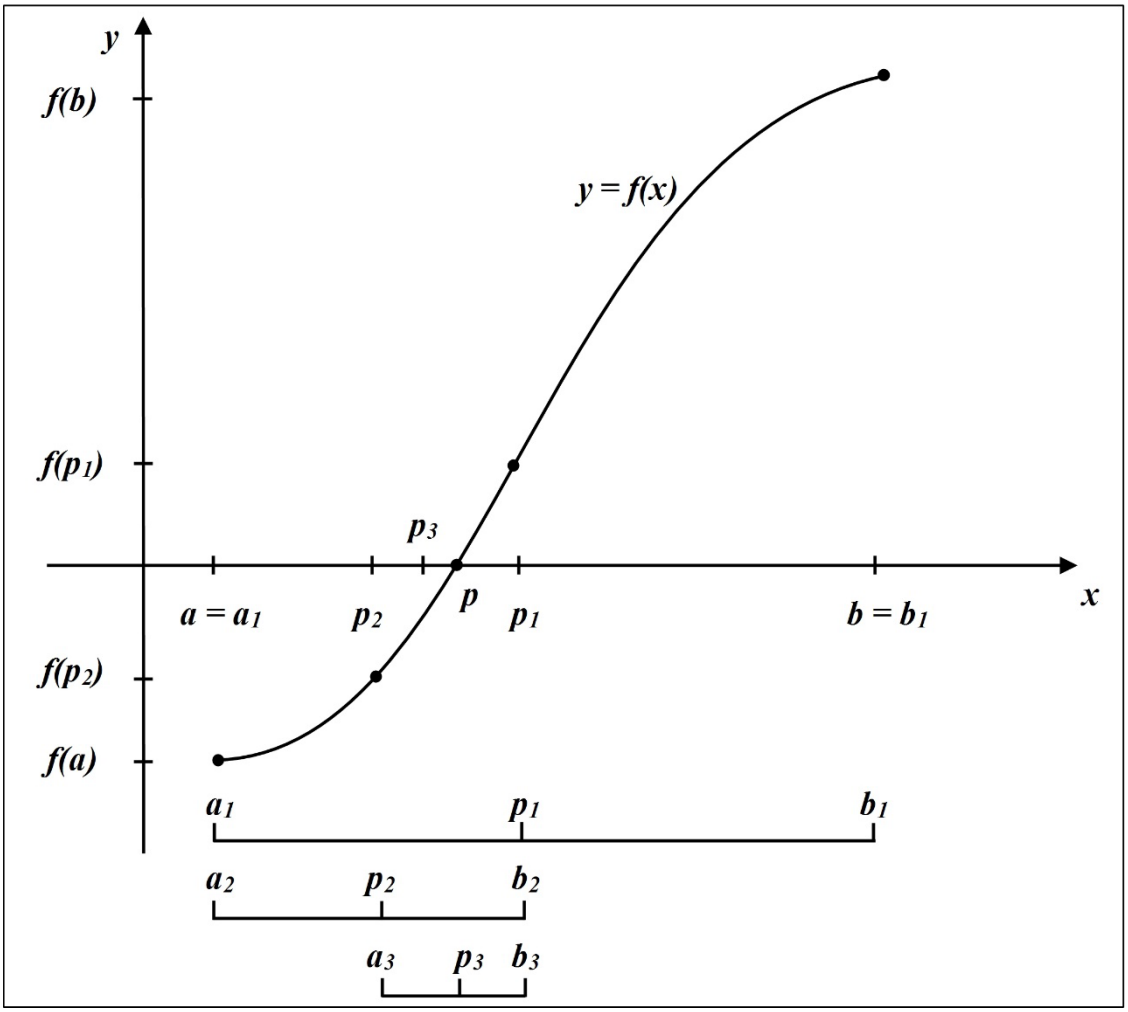

Figure 5.6 Bisection method converge at $f(x) = 0$

5.4.2 Application of bisection method for estimation of interphase permittivity

Fixing extreme bounds for unknown relative permittivity is the first step to start-off proposed algorithms. Bisection method begins by assigning a = 0.0000000001 and b = 10 as lower and upper bound respectively to interphase relative permittivity. For the specific value of interphase thickness, following iterative steps are continued till a converged solution for interphase relative permittivity is obtained.

Step 1: Calculate the value of p (i.e midpoint of the interval), $p = (a + b)/2$.

Step 2: Change the permittivity value of interphase layer in COMSOL model to p. Simulate the model and determine the effective permittivity of the model (composite material). Store the effective permittivity of composite material in ε_r_NC_Simulated.

Step 3: If (ε_r_NC_Simulated $-$ ε_r_NC_Measured) > 0, then assign the value of p to a; If (ε_r_NC_Simulated $-$ ε_r_NC_Measured) < 0, then assign the value of p to b; now the solution interval bisected to either a to p or p to b. where ε_r_NC_Measured is the measured value of permittivity (experimental data) obtained from dielectric spectroscopy.

Step 4: If (ε_r_NC_Simulated $-$ ε_r_NC_Measured) is less than the tolerance limits (0.001), and then the solution is converged. Fix the interphase permittivity of nanocomposite at p for the particular value of interphase thickness. ε_r_Interphase = p.

Step 5: If the solution does not converge, go to step 1 with the updated interval. ε_r_NC_Measured.

This algorithm is depicted using a flow chart shown in Figure 5.7. All the variables associated with the flow chart are elaborated in Table 5.3.

Table 5.3 List of variables used in the flowchart

Variables	**Description**
runtime	Used to choose one from the16 available frequencies
Frequency	Current simulation frequency
Frequency(runtime)	Frequencies at which experimental data are available
ε_r_Interphase	Permittivity of interphase
ε_r_Interphase_Final (runtime)	To store final converged value of interphase permittivity
ε_r_NC_Simulated	Permittivity of NCs obtained through simulation
ε_r_NC_ Measured	Measured permittivity value of NCs chosen for the current iteration
ε_r_NC_ Measured(runtime)	Measured permittivity value of NCs corresponding to 16 different frequencies
lowbound	Lower bound variable of bisection method
upbound	Upper bound variable of bisection method
mean	Midpoint of lower and upper bound

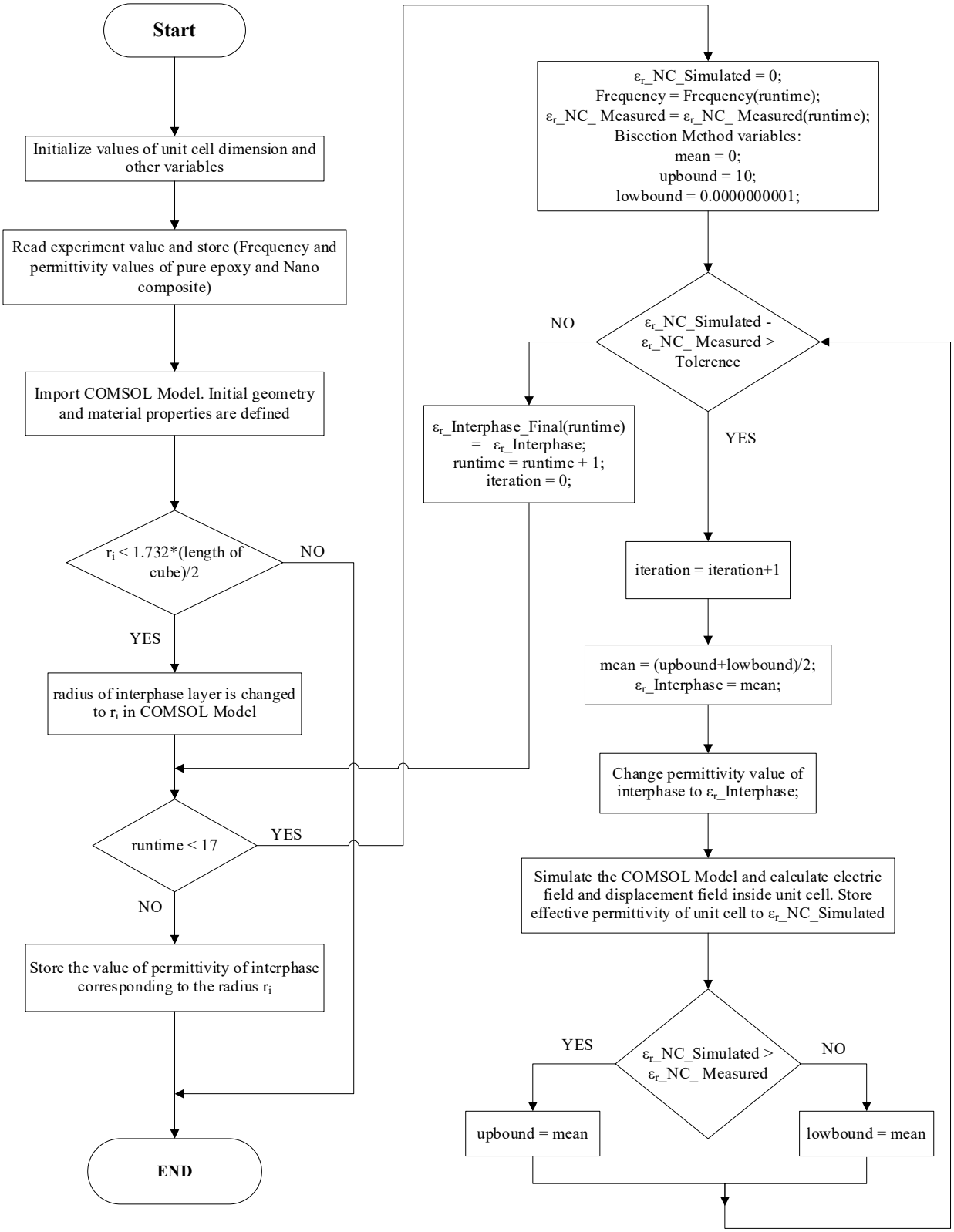

Figure 5.7 Flowchart to calculate permittivity of the interphase

5.5 DISCUSSION ON IMPORTANT FINDINGS

Finite element analysis is carried out in accordance with the process demonstrated in Figure 5.1. Post-processing is carried out to derive electric field intensity and electric flux density from nodal potentials. Typical solutions for electric field intensity and electric flux density are shown in Figure 5.3. The relative permittivity of nanocomposites is estimated from electrostatic field parameters (i.e., electric field intensity and electric flux density) following methods discussed in section 5.2. Relative permittivity of the interphase is obtained following the computation processes described in section 5.4. Estimated values of interphase permittivity value over a frequency range of 10^{-2} to 10^{7} Hz for various assumed interphase thicknesses is shown in Figure 5.8. For entire frequency range relative permittivity of interphase is pressingly lower than the permittivity of neat polymer to provide a best fit of measured and computed effective permittivity of the nanocomposites. As seen in Figure 5.8, multiple combinations of interphase thickness and permittivity are possible to achieve a converged solution. A screening of the simulated results is needed to decide the best representative values of interphase parameters (size and permittivity) for the chosen material. Epoxy alumina nanocomposite is solid dielectrics with three constituent phases (i.e., host, filler, and interphase). Under the influence of electric field solid dielectrics are polarizable so the constituent phases. Thus, the interphase permittivity can't be lower than 1, which implies that interphase thickness is greater than 10 nm. All polarization mechanism (atomic, ionic, dipolar and interfacial/space charge) shows their contribution on dielectric response at different time scale. As the frequency decreases cumulative contribution of different polarization mechanism increases. Thus, permittivity of interphase is expected to exhibit a frequency response similar to that of neat polymer and nanocomposites. It may be noted that only for interphase thicknesses greater than

40 nm, the interphase permittivity shows an expected trend (more specifically, in the low frequency regime). In order to settle on a unique value for interphase permittivity further screening has been carried out. At constant frequency of 50 Hz, the measured relative permittivity of nanocomposite and estimated relative permittivity of interphase for a range of thicknesses from 10 nm and 150 nm is shown in Figure 5.9. It is observed that any change in interphasial region affect the effective permittivity of composites only up to an interphase thickness of 100 nm. Extending interphase region beyond 100 nm has no effect on the estimate of interphase permittivity. For an interphase thickness of 50 nm measured permittivity of nanocomposites and corresponding simulated interphase permittivity is shown in Figure 5.10a. A similar plot for an interphase thickness of 100 nm is shown in Figure 5.10b. Clearly, difference between interphase permittivity and permittivity of nanocomposites is insignificant at an interphase thickness of 100 nm. Typical interphase region in a unit cell is highlighted in Figure 5.11a. Computed interphase volume fraction for different interphase thickness is shown in Figure 5.11b. It is important to stress that for filler concentrations of 1 vol.% interphase volume fraction is maximum at an interphase thickness of 100 nm. For thicknesses below 100 nm, the permittivity of composites is dependent on all three-constituent phase i.e., base polymer, filler, and interphase. On the other hand, at an interphase thickness of 100 nm, base polymer is completely transformed to interphasial polymer, and the effective permittivity of composites is predominantly governed by the permittivity of interphase. It implies that interphase permittivity will assume a value that is bordering to the measured permittivity of nanocomposites.

According to Raetzke and Kindersberger [97] the interphase formed around the nanoparticles is responsible for enhanced material properties. For certain interphase thickness, a maximum of interphase volume may be achieved at a distinct filler loading.

If dielectric properties are measured at different filler loadings, the maximum deviation in the properties of nanocomposites with respect to the neat polymer are achieved at a filler loading at which the interphase volume fraction is maximum. Different dielectric spectroscopic measurements in the literature reveal that polymer nanocomposites may exhibit lower relative permittivity than that of the neat polymer at low filler concentrations [99], [100], Large section of the literature attribute permittivity change in nanocomposites to local change in polymer structure at interfaces which influence chain dynamics or mobility of the polymer chain. Our measurements exhibit maximum change in the dielectric properties at a filler content of 1 vol.%. The interphase thickness that maximizes interphase volume fraction at that filler content is 100 nm. This supports our hypothesis that the interphase thickness for the investigated material extends up to 100 nm and attains a relative permittivity of 3.73 at 50 Hz.

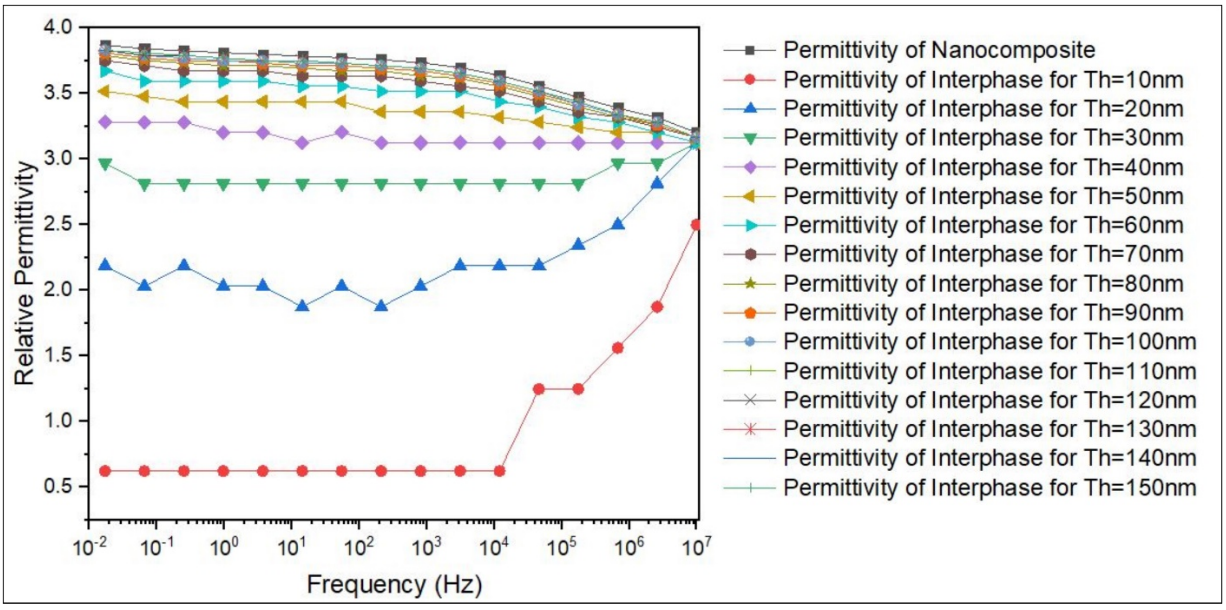

Figure 5.8 Estimated interphase permittivity and interphase thickness required get the solution converged.

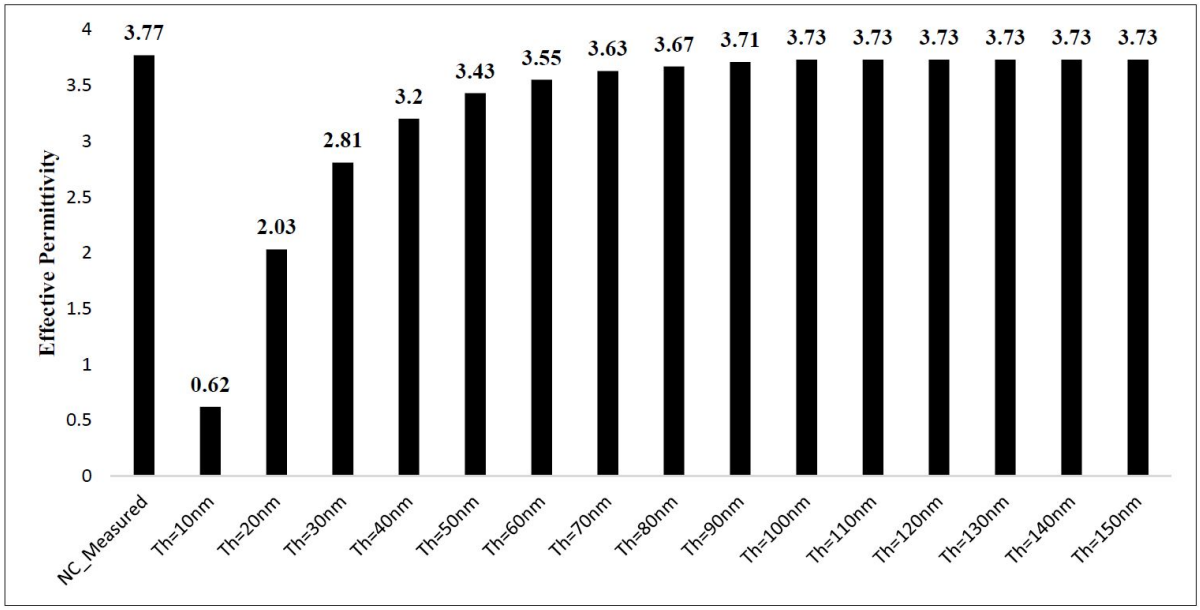

Figure 5.9 Relative permittivity of nanocomposite and interphase at power frequency 50 Hz corresponding to interphase thickness.

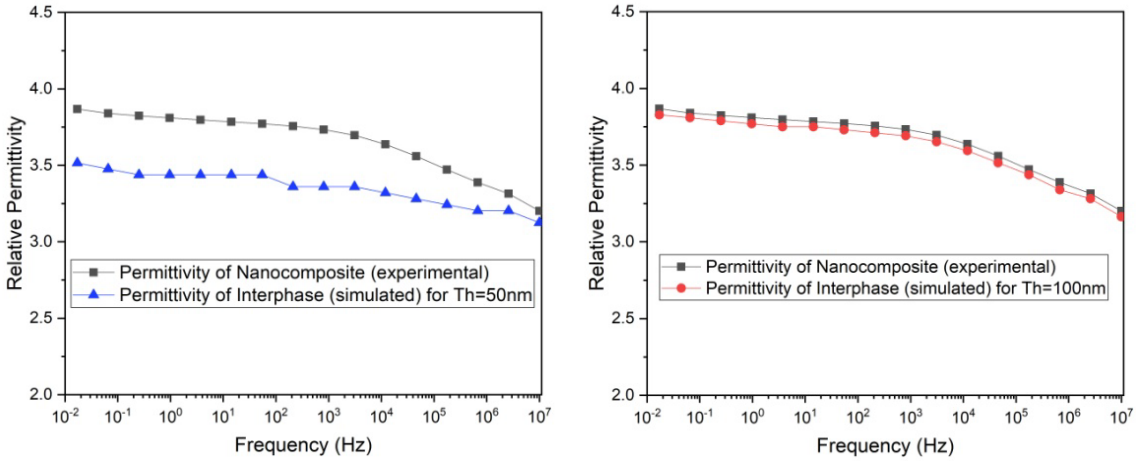

(a) (b)

Figure 5.10 Interphase permittivity obtained thorough the simulation model and measured permittivity of nanocomposites sample (a) interphase thickness of 50 nm (b) interphase thickness of 100 nm.

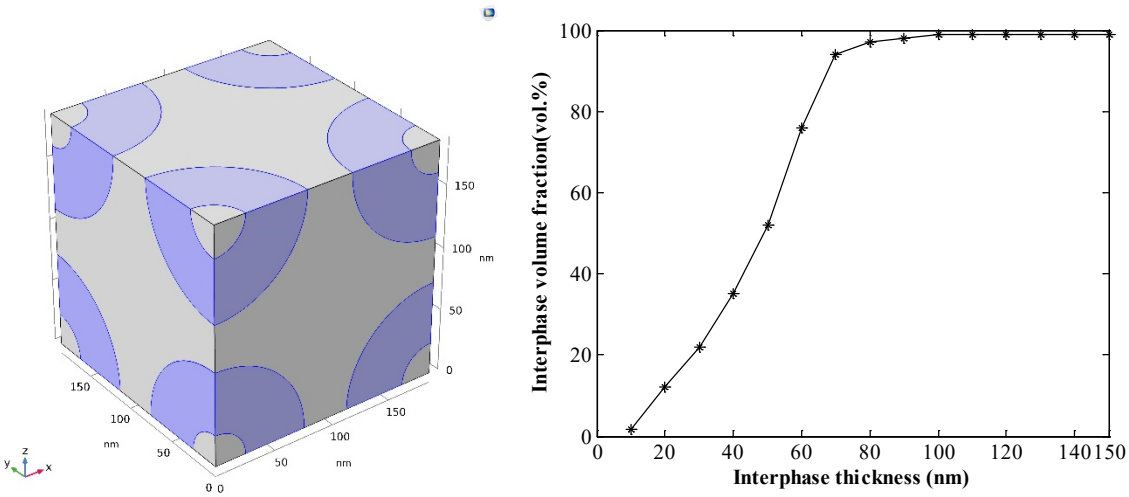

(a) (b)

Figure 5.11 Interphase (a) highlighted region in unit cell (b) computed interphase volume fraction for different interphase thicknesses.

The proposed method is effective in estimating interphase parameters (size and permittivity) with underlying assumption that all filler particles are of same size (i.e. 50 nm). Any scatter in particle size may affect the accuracy of the model. Prediction by numerical model is linked to experimental results, which are affected by variability in the particle size and shape. In the present study filler shape is spherical. Studies may be carried out with other filler shape e.g. layered silicates [101]. Msekh et al. [101] conducted simulation studies to predict tensile strength and fracture toughness of fully exfoliated nanosilicate clay epoxy composites using phase field model. Their findings also suggest that interphase thickness is a dominant parameter that governs the tensile strength of the nanocomposites. Nevertheless, length scale in their model is one order lower than used in the current study. Few researchers speculated that the interphase region in polymer nanocomposites may extend from couple of nm to few hundreds of nm [97], [102]. The extent of interphase may vary on account of variability in chosen base polymer, filler material, and filler surface functionalization.

5.6 SUMMARY

The interphase in epoxy alumina nanocomposites is quantified using simulations in conjunction with dielectric spectroscopic measurements. To determine the extent of interphase and its permittivity in epoxy alumina nanocomposites, a novel bisection-based algorithm is proposed. The interphase in epoxy alumina nanocomposites is observed to extend up to 100 nm, and its relative permittivity is slightly less than the composites' effective permittivity. The proposed method will aid in determining the optimal amount of nanofillers to use in order to obtain the best dielectric properties for polymer nanocomposites. Additionally, the proposed method is applicable to the prediction of other properties pertaining to interphase in polymer nanocomposites. The following chapter will describe a method for estimating thermal conductivity of interphase in epoxy alumina nanocomposites.